Classification of Resampled Pediatric Epilepsy EEG Data Using Artificial Neural Networks with Discrete Fourier Transforms

Temel Sonmezocak*, Gizem Guler, Merih Yildiz
Department of Electrical and Electronics Engineering, Dogus University, 34775 Istanbul, Turkey
**tsonmezocak@dogus.edu.tr; 202291073005@dogus.edu.tr; myildiz@dogus.edu.tr*

***Abstract*—Epilepsy is a neurological disorder commonly observed in children. Currently, electroencephalography (EEG) is widely used as the most important diagnostic method for epilepsy in medical practice. The diagnosis of epilepsy in pediatric patients is challenging due to their high level of activity and incomplete brain development. In this study, data sampled at 256 Hz were obtained from patients between the ages of 7–12, collected by Boston Children's Hospital. First, the image intervals that contain seizure waves were identified in the datasets, and the discrete-time Fourier transform (DFT) was applied. The amplitude-frequency features of the frequency spectrum in seizure and nonseizure states were obtained, and patients were classified for seizure detection using a multilayer perceptron (MLP) based on an artificial neural network (ANN) architecture. In the next step, the EEG signals were resampled at low frequencies, and the same analyses were repeated to minimise the disadvantages of limiting factors such as storage space and processing power, resulting in reduced storage space usage and more efficient performance.**

***Index Terms*—Electroencephalography; Epileptic seizure; Discrete transforms; Machine learning.**

I. INTRODUCTION

Epilepsy is a chronic condition that affects more than 50 million people worldwide and requires long-term follow-up. It commonly manifests as epileptic seizures due to sudden and abnormal discharge of nerve cells from the brain [1]. These seizures can occur in different types and vary in response to treatment from person to person. There is no difference in incidence between males and females. Epilepsy is frequently observed in childhood, typically presenting in the early years of life and causing intellectual disability, learning difficulties, and hyperactivity disorder in 25 % of affected children [2].

Electroencephalography (EEG) is an imaging technique that is used in the diagnosis and determination of the type of epilepsy, as well as in the diagnosis of many other neurological disorders. In adults, EEG measurements can easily be obtained compared to those of child patients, as the brain has completed its development. This allows seizure conditions to be identified. Electrical activities in the brain change with age. Due to the mobility of children and the fact that their brain development processes have not yet been completed, interpreting EEG recordings of child patients is more difficult than that of adult patients and requires careful interpretation by pediatric neurologists [3].

In high-income countries (HICs), there are few difficulties in accessing hospital equipment and specialised physicians, while low- and middle-income countries (LMICs) often lack these resources. For example, in 2017, there were only 208 neurologists working in Colombia, which means that there was only one neurologist per 240,000 people. Statistical studies by the health department estimate that there will be a maximum of 629 neurologists in the country by 2030, which is still an insufficient number [1]. Given this situation in LMICs, digital transformation in epilepsy diagnosis is greatly needed to reduce the time neurologists spend reviewing EEG images. The minimum time required to interpret the EEG images is between 30 and 60 minutes, significantly limiting the number of diagnoses a neurologist can make in one day. With the help of machine learning algorithms, much faster and more accurate results can be obtained [2]–[4].

When studies on the EEG signal classification are examined in this context, machine learning algorithms based on EEG data from childhood epilepsy patients have been applied to various classification methods in recent years, particularly using deep learning models based on different convolutional neural network (CNN) architectures to predict epileptic seizures in advance [5]. With these CNN architectures, 95 % accuracy can be achieved with AlexNet and 94.17 % with GoogleNet [1]. In another study, resampling techniques were investigated to reduce the effect of motion artifacts on EEG signals. Here, a K-nearest neighbour (KNN) algorithm was used to obtain a 0.98 area under the curve (AUC) rate and a 98.4 % accuracy rate [6]. However, these studies need to go further to make a more efficient and rapid diagnosis of pediatric epilepsy seizures with less storage space. Therefore, in this study, a new method is proposed based on resampling of childhood epilepsy EEG data in lower frequency ranges (128 Hz–64 Hz) according to the Nyquist theorem [7] is proposed. Frequency spectra were obtained using a discrete-time Fourier transform (DFT) for the resampled samples in the proposed study. Feature reduction was performed by determining the mean frequency (MNF) characteristics from the obtained spectra. Classification was performed using the

Manuscript received 18 July, 2023; accepted 25 October, 2023.

obtained values together with an artificial neural network (ANN) architecture based on multilayer perceptron (MLP) structure, particularly effectively determining seizure and nonseizure conditions in child patients. Additionally, the proposed system is efficient in terms of processing speed while using even less storage space.

II. MATERIAL AND METHOD

A. Electroencephalography

EEG was first recorded in 1924 by the German psychiatrist Hans Berger. Between 1929 and 1938, he published numerous research articles on EEG [8]. EEG signals are a continuous signal consisting of the oscillation of potential differences over time. EEG graphs are plotted as voltage signals over time. Each signal is the instantaneous value of the voltage in equally spaced time intervals [9]. EEG is an imaging method that records electrical signals generated by neurons through small electrodes placed on the scalp using a gel. The most common electrode placement technique is the international 10-20 system, which involves placing 21 electrodes around the circumference of the skull shown in Fig. 1 [10].

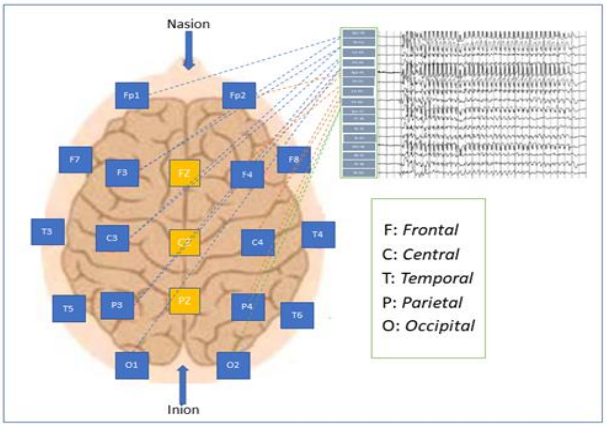

Fig. 1. Positions of electrode placement according to the international 10-20 system.

Brain waves are divided into four main categories: alpha, theta, delta, and beta waves shown in Fig. 2.

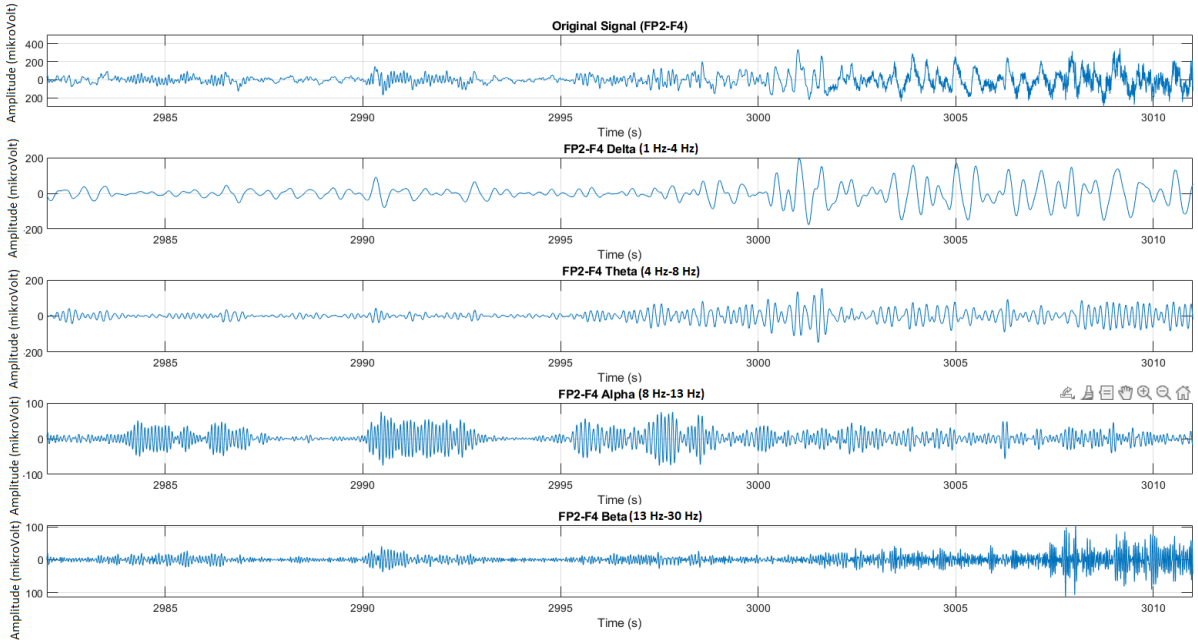

Fig. 2. EEG signal obtained from different frequency regions of the FP2-F4 channel of an 11-year-old girl showing the moment of epileptic seizure.

Beta waves (12 Hz–30 Hz) typically occur during wakefulness and intense thinking and have a high frequency. Alpha waves (8 Hz–12 Hz) are typically seen in a relaxed mental state and have a lower frequency. Theta waves (4 Hz–8 Hz) are typically seen during light sleep. Delta waves (0.1 Hz–4 Hz) are the waves with the lowest frequency and are typically seen during deep sleep. Human EEG largely contains signal power in the 1 Hz–30 Hz frequency range. There is some evidence that higher frequencies may also carry important neurophysiological information. However, most EEG studies are concerned with EEG signals in the 1 Hz–30 Hz frequency range [11].

The effect of epileptic seizures on brain waves can vary depending on the type of seizure and the overall condition of the patient. Therefore, in this study, all channels for each patient are analysed in all frequency ranges, and the distinctive features of the frequency spectra are examined for effective classification.

B. Dataset

In this study, a total of 844 hours of EEG data were used from 9 pediatric patients with ages ranging from 7 to 12 years (Table I), which were made publicly available by Boston Children's Hospital-MIT, were used. The recordings for each patient consisted of EEG data sampled at 256 Hz from 16 different channels.

TABLE I. PATIENT DEMOGRAPHICS IN THE DATASET.

Patient No.	Gender	Age
1	F	11
2	M	11
3	F	7
4	F	10
5	F	12
6	F	9
7	F	9
8	F	7
9	F	12

C. Signal Preprocessing

In EEG devices, signals are typically passed through analogue filters, as seen in Fig. 3, before being converted into digital signals. This process eliminates noisy frequency components and obtains the desired frequency components. For example, a high-pass filter suppresses low-frequency signals (typically signals below 0.1 Hz) and passes high-frequency signals (typically signals above 50 Hz). Similarly, low-pass filters suppress high-frequency signals and pass low-frequency signals. In addition, some modern EEG devices use digital filters. Unlike analogue filters, these filters primarily process recorded signals digitally to improve signal quality. Other advantages of these filters include the ability to change filter parameters, better frequency options, and greater sensitivity of the filter [12].

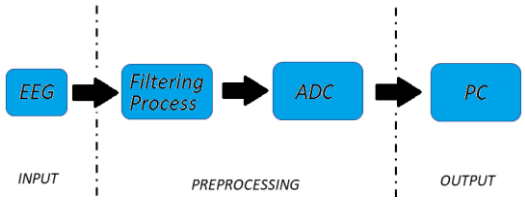

Fig. 3. The preprocessing process of EEG devices signal.

Significant frequency ranges for epilepsy diagnosis in EEG datasets are up to 30 Hz [10]. Therefore, the alpha, theta, delta, and beta frequency ranges were taken into account for the 256 Hz sampled signals of each patient, and all of these signals were filtered using second-order Butterworth low-pass digital filter structures to eliminate high-frequency components in the EEG data. Additionally, the same EEG dataset was resampled at 128 Hz and 64 Hz frequencies [13]. During this process, the minimum sampling frequency was chosen at least twice the frequency limit of the Beta band, following the Nyquist theorem [7], to avoid any data loss.

D. Obtaining Frequency Features Using DFT

The Fourier transform (FT) expresses an exponential function with frequency f and time variable t in seconds as a periodic function of the form $e^{\pm j2\pi ft} = cos(2\pi ft) \pm jsin(2\pi ft)$. From this all sinusoids with frequencies that make up the original signal can be obtained. The Fourier transform is applied to nonperiodic continuous signals. However, when processing discrete-time data, the discrete-time Fourier transform (DFT) considers time intervals discretely and calculates frequency components by sampling the data at equal intervals, assuming that the data are periodic. As a result, the distinction between frequency components increases and the frequency components of the signal are more accurately identified. Therefore, in this study, DFT is preferred over FT.

DFT represents a signal as a combination of complex exponentials known as frequencies [14] with discrete sampling consisting of equidistant N point. $s[n]$, represented as $s[0]$, $s[1]$, $s[2]$,…, $s[N - 1]$. In other words, in this transform, the given signal is considered as a periodic signal and applies this signal over a period of N. Applying DFT to $s[n]$ generates another sequence $s[k]$. When DFT is applied to the data sequence $s[n]$, the resulting sequence is given by $s[k]$ as obtained in (1) [15]

$$s[k] = \sum_{n=0}^{N-1} s[n] e^{\left(-\frac{j2\pi kn}{N}\right)}. \quad (1)$$

In (1), for each $s[n]$ where $n = 0, 1, 2, ..., N - 1$, the value of $s[k]$ represents the frequency-domain output of each k^{th} component as a complex number $(a + jb)$. The imaginary part of $s[k]$ contains the phase information of the signal [16], [17]. In the literature, $s[k]$ is commonly referred to as the spectrum domain. The length of $s[k]$ is expressed as 0 to $N/2$. As with the time-domain axis, the frequencies also periodically repeat from 0 to the data sampling frequency (Fs). Therefore, as a result of this periodicity, it corresponds to (2)

$$s[k] = s[k+N] = \sum_{n=0}^{N-1} s[n] e^{-j\frac{2\pi}{N}(k+N)n} = \sum_{n=0}^{N-1} s[n] e^{-j\frac{2\pi}{N}kn}. \quad (2)$$

The sampling period of the DFT is $n\Delta t$ (Δt: *sampling interval*). As seen in the above equation, the ratio k/N corresponds to the sampling interval per cycle [14], [16]. After $k = N/2$, the magnitude value repeats itself, but not in terms of the direction of the signal. The DFT transformation of an analogue signal, beyond the Nyquist frequency, is essentially in complex conjugate form. In other words, for $k > 0$, $s[k] = s[N - k]^*$. Frequencies beyond $Fs/2$ are not included because negative frequencies are of the same magnitude as positive frequencies and the entire cycle repeats after N points.

In the DFT process, the total observation time of the signal is considered as $N\Delta t$ [17]. The k^{th} value in the DFT, F_k, is determined based on the relationship between the sample number N and Δt [17], [18]

$$F_k = \frac{k}{N\Delta t}. \quad (3)$$

In (1), (2) and (3), the first DFT result corresponds to 0 *Hz* ($k = 0$), which is equal to the sum of all signal values. For the 2^{th} frequency ($k = 1$), $F_1 = 1/N\Delta t$. This continues until $k = N/2$. In other words, this point is half of the sampling frequency, which corresponds to the Nyquist frequency at $Fs/2$. Frequencies beyond this point, including the Nyquist frequency, are displayed on the negative frequency axis. All these features related to the DFT process are summarised in Fig. 4 as an example.

	Signal array with N points (Sampling interval Δ t)					
Signal s[n]	s[0]	s[1]	s[2]	s[3]	...	s[N-1]
Data No.	1	2	3	4	...	N
n index	0	1	2	3	...	N-1
Sampled time	0	Δt	2Δt	3Δt	...	nΔt
	DFT output of N points					
DFT of Signal s[k]	s[0]	s[1]	s[2]	s[3]	...	s[N-1]
Data Output No.	1	2	3	4	...	N
k index	0	1	2	3	...	N-1
Frequency	0	1/NΔt	2/NΔt	3/NΔt	...	k/NΔt
	0	F	2F	Fs/2	-2F	-F
		Positive frequencies		Nyquest frequency	Negative frequencies	

Fig. 4. Explanation of the DFT output data with 6 points as an example.

In this study, raw EEG signals sampled at 256 Hz in the time domain were digitally filtered and then resampled at

256 Hz, 128 Hz, and 64 Hz to obtain the $s[n]$ samples, which were then transformed into instantaneous frequency $s[k]$ values at discrete time intervals using DFT. In the next step, to increase the speed and efficiency of the machine learning process before classifying epilepsy seizures, a feature reduction [19] was performed. In this process, mean frequency (MNF) values were obtained from the magnitudes of instantaneous frequencies at each discrete time

$$MNF = \sum_{j=1}^{M} f_j P_j \Big/ \sum_{j=1}^{M} P_j . \quad (4)$$

MNF is the average frequency value of each instantaneous frequency value obtained by multiplying the power spectrum density values of the signal at each instantaneous frequency value for $J = 1, 2, ..., M$ and summing them up, divided by the same power spectrum density values of the spectrum [20]. In (4), f_j represents the frequency of the j^{th} frequency band, P_j represents the power spectrum of the signal in the j^{th} frequency band, and M represents the length of the frequency band.

E. Classification of Epileptic Seizure States Using MLP

Artificial neural network (ANN) is a machine learning method developed from the idea of simulating the human brain. Artificial neurons are the building blocks of this system. ANN is used to solve many problems in machine learning, such as learning, classification, prediction, data compression, image processing, natural language processing, and more. It is formed by connecting many nodes or neurons shown in Fig. 5. These neurons process input data and generate outputs. ANN automatically adjusts its weights ($W: 1, 2, \ldots, m$) during the learning process by taking examples ($input: 1, 2, \ldots, m$) from the data sets. This allows the automatic discovery of the necessary features for a model to perform better [21].

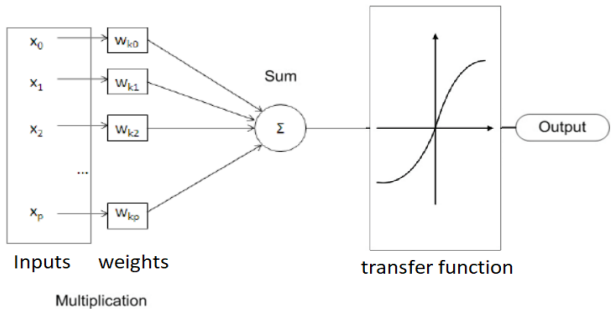

Fig. 5. Example of an artificial neuron model.

As the size and complexity of data sets increase, artificial neural networks perform better. One of the most popular methods used to evaluate EEG signals is the neural network models. Therefore, the multilayer perceptron (MLP) architecture based on the forward propagation algorithm, which is the most widely used artificial intelligence algorithm for classification, was preferred in this study [22]. Additionally, it provides more variable parameters compared to other artificial intelligence algorithms. In this study, the adaptive moment estimation (Adam) optimization was used to train artificial neural networks and optimise deviations. This algorithm requires less memory since it does not need to store all the gradient history like other optimisation algorithms [23], is computationally efficient, and is suitable for complex models dependent on large data sets. The data sets in the study were divided into 80 % training and 20 % testing. Additionally, the model created to improve the effectiveness of the training process was trained by grouping it with cross-validation at different K-fold values. This validation method is particularly used for the effective performance of the model during machine learning [4]. The most effective performance value obtained from the model we created in this study is achieved at K-fold: 5.

The MLP structure created consists of three layers: the input layer, the hidden layer, and the output layer. The activation function used for neurons in the input layer is the sigmoid function shown in (5)

$$f(x) = 1/(1+e^{-x}). \quad (5)$$

Here, x is the input value given to the sigmoid function. The output values range between *0* and *1* [24]. This function *f(x)* is particularly used in classification problems and limits the output of neurons. The reason for using the sigmoid function in this study is that EEG signals consist mainly of low-frequency signals [25]. For the activation of neurons in the output layer, SoftMax was used. Using the SoftMax function in the last layer for the classification of EEG signals, the probability of each class is effectively calculated. The SoftMax function normalises the outputs to ensure that their sum is equal to 1 [26]. Table II shows the parameters of the constructed neural network model.

TABLE II. ANN MODEL PARAMETERS OF THIS STUDY.

Data Set Rate (%)	80 % training, 20 % test
Input Layer Activation Function	Sigmoid
Output Layer Activation Function	Softmax
Learning Rate	0.01
Optimisation Algorithm	Adam
Epoch	500
K-fold	5

Finally, in the classification process, data consisting of the MNF features of EEG signals with and without seizures in patients were divided into two classes using the open source Fieldtrip toolbox, MATLAB-based software [27], and classification accuracy (%) and area under curve (AUC) metrics were used to evaluate performance [28]. The accuracy rate represents the ratio of correctly classified examples and is calculated as shown in (6) [29]

$$Accuracy(\%) = \frac{1}{N}\sum_{k=1}^{N}\left\lfloor \frac{NCCS}{TNS} \right\rfloor \times 100. \quad (6)$$

where N is the number of classes, $NCCS$ is the number of correctly classified samples, and TNS is the total number of samples. The AUC value, on the other hand, represents the area under a ROC curve and is a commonly used metric to measure the performance of a classification model. AUC measures the accuracy of the classification model, i.e., its ability to correctly separate positive and negative examples, and its value ranges from *0* to *1*. The closer it is to *1*, the better the performance of the classification model [28], [29].

III. RESULTS

The frequency spectra of the EEG recordings were obtained, including all channels of the patients. Figure 6 shows the spectra of 3 different patients as an example, where the densities represented by the light colours in the power spectra are particularly observed during seizure states for each patient. The frequencies corresponding to these densities represent the seizures frequencies and are typically below *10 Hz* for all patients (Fig. 6(a)). In nonseizure states, the amplitudes of low-frequency components are observed to be quite low (Fig. 6(b)).

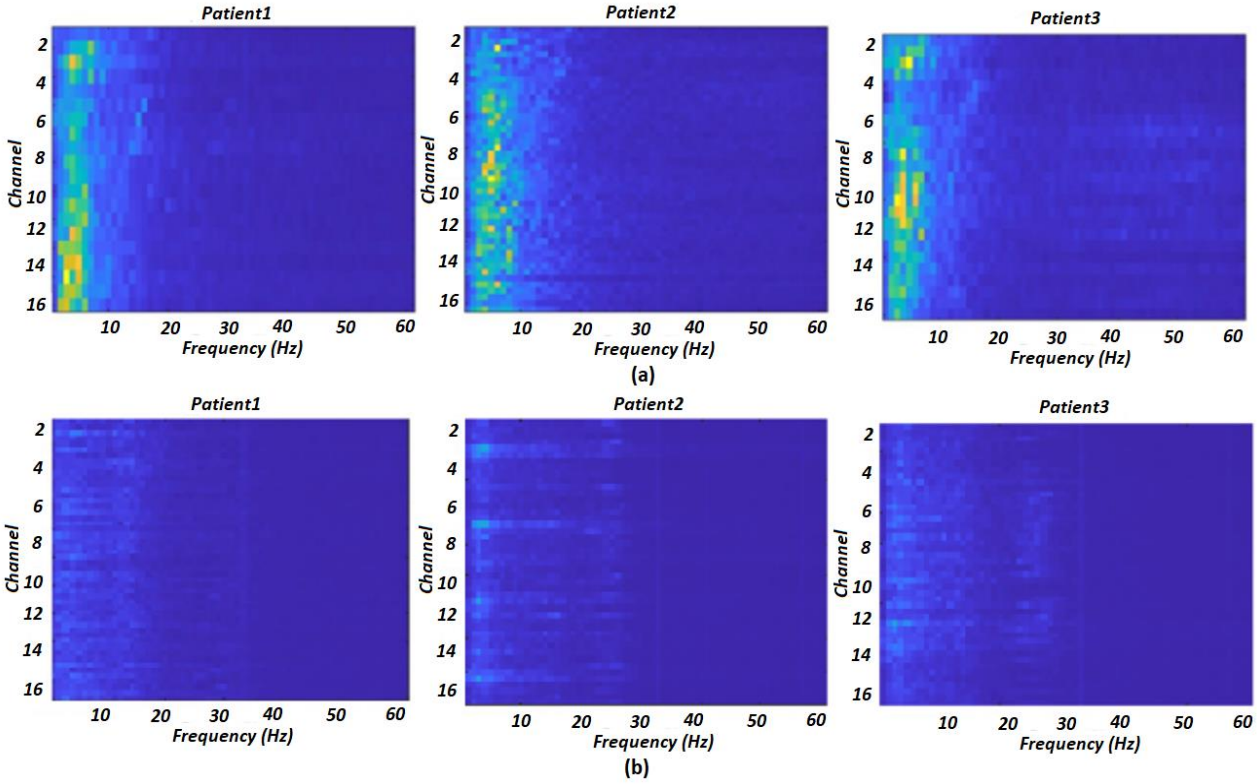

Fig. 6. Frequency spectrum: a) Seizure status; b) Nonseizure status.

However, to increase the speed and efficiency of the machine learning process before classifying epilepsy seizures using instantaneous frequency values, a feature reduction process [19] is performed. In this process, mean frequencies (MNF) are obtained from the instantaneous frequency magnitudes at each discrete time. 80 % of the data containing these feature values were used for training, while the remaining 20 % were allocated for testing. The data containing these feature values were divided into two classes, seizure and nonseizure states, and classified using MLP. The performance results obtained from the classification are presented in Fig. 7, Tables III and IV.

Figure 7 shows the performance graphs of accuracy (%) and the error rate obtained from the MLP trained on the resampled signal (Fs: 64 Hz with K-fold: 5). When examining this graph, it can be observed that the accuracy value is 98.85 % and the error rate is below 0.1. Furthermore, the same study was repeated with different K-fold values shown in Table III.

Table III shows the accuracy (%) values obtained from different K-fold values for data containing MNF features sampled at a resampling frequency of 60 Hz (80 % training, 20 % test). The highest accuracy rate is obtained at K-fold: 5, as can be seen from this table. Therefore, K-fold: 5 is selected and the system performance is investigated for different resampling frequencies. For the system's performance, AUC parameters are examined this time. The results are presented in Table IV.

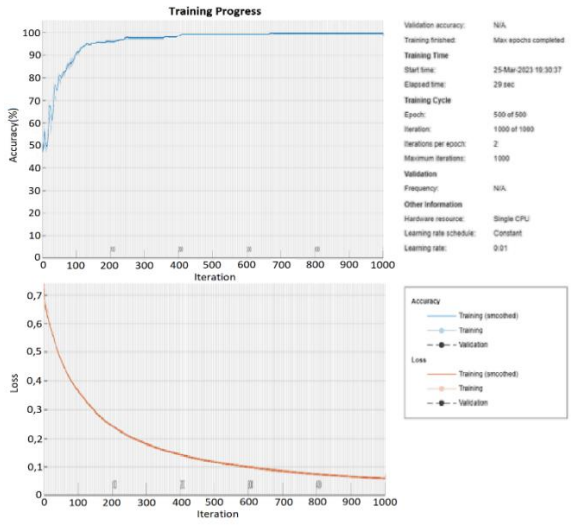

Fig. 7. Accuracy performances & loss rates for K-fold:5.

TABLE III. ACCURACY PERFORMANCES OF MLP FOR DIFFERENT K-FOLD.

K-Fold Value	Resampling Freq. (Hz)	Accuracy (%)	K-Fold Value
Fold 1	64 Hz	95.40 %	Fold 1
Fold 2	64 Hz	94.32 %	Fold 2
Fold 3	64 Hz	96.59 %	Fold 3
Fold 4	64 Hz	94.32 %	Fold 4
Fold 5	64 Hz	98.85 %	Fold 5

TABLE IV. AUC PERFORMANCE VALUES OBTAINED FROM DIFFERENT RESAMPLING FREQUENCIES.

Resampling EEG Data	Resampling Freq. (Hz)	AUC Parameters
Raw EEG Data	256 Hz	0.9932
Resampled EEG Data	128 Hz	0.9934
Resampled EEG Data	64 Hz	0.9952

As shown in Table IV, the AUC value close to 1 indicates excellent performance. In fact, it is clear from this table that even better results were achieved by resampling at lower frequencies compared to the results obtained with the original frequency of 256 Hz. Although a closer to 1 result is obtained at lower frequencies, samples at much lower frequencies were not included in the study due to the Nyquist theorem [7], which requires the maximum frequency in the significant frequency range to be at least twice the sampling frequency to avoid aliasing effects. Since the frequency range of interest in this study was up to 30 Hz, sampling at a frequency of 64 Hz was considered due to the Nyquist theorem.

IV. DISCUSSION

In recent years, various classification methods have been developed based on EEG data from childhood epilepsy patients. In particular, deep learning models based on different architectures of convolutional neural networks (CNNs) have been used to predict epileptic seizures using EEG signals, achieving accuracy performances of 95 % with AlexNet and 94.17 % with GoogleNet [1]–[5]. However, CNN structures based on the deep learning approach, especially, process signals in 2-dimensional format [30]. Therefore, performing complex and time-consuming 2D signal processing on EEG signals can be a computationally demanding task. In recent literature, studies are also being conducted using normal machine learning classification methods for EEG signals [31], [32]. These studies have achieved classifier performance at levels of 98.4 % and 0.98 AUC [6].

However, the sampling frequencies for raw EEG data are generally in the range of 256 Hz. In this study, a model is proposed focussing on fast processing and effective evaluation of raw EEG data sampled at 256 Hz, which is different from other studies. When examining Tables III and IV, the proposed model shows particularly high efficiency, with 98.85 % accuracy and 0.9952 AUC. This model is based on an artificial neural network (ANN) architecture, specifically a multilayer perceptron (MLP) model, and utilises feature reduction based on reducing the instantaneous frequency values obtained from the discrete-time Fourier transform (DFT) to the mean frequency (MNF), taking into account only the frequency intervals in which childhood epilepsy seizures are observed and resampling at a lower frequency (e.g., 64 Hz) in lower frequency ranges. This model is a contribution to the literature.

This allows for a reduction in the number of samples that need to be processed through resampling, thereby reducing the computational complexity involved in processing EEG signals. Furthermore, when used in conjunction with feature reduction, it reduces the dimensionality of data, requiring less memory and computational power for the storage and processing of EEG signals. Resampling at low frequencies can increase the time resolution of EEG signals, allowing for better tracking of rapid changes in the signals. It can also help smooth out high-frequency noise or other unwanted signals, thus reducing or eliminating distortions in the signal and obtaining a better signal-to-noise ratio. Changing the sampling frequency of EEG signals can accommodate different processing techniques or analysis methods. It can also align different EEG signals from different sources or devices to the same sampling frequency, making them compatible with each other [12]. In this study using resampling, considering the age-related changes in electrical brain activities and the fact that EEG recordings of child patients are more difficult to interpret than those of adult patients due to child movement and incomplete brain development, careful interpretation by child neurologists is required [3]. Moreover, in low- and middle-income countries, digital transformation in childhood epilepsy diagnosis is also important to reduce the time it takes for neurologists to review EEG imaging.

V. CONCLUSIONS

In this study, raw EEG recordings sampled at 256 Hz from 9 patients aged between 7 and 12 years of age obtained from Boston Children's Hospital were processed by resampling the signals at the same frequency of 256 Hz and then again at lower frequencies. The results were compared in a comparative analysis.

All resampled samples were processed using the DFT to obtain instantaneous frequency values generated in discrete time and then reduced to MNF features. The resulting MNF features were effectively classified using ANN-based MLP structures, achieving 98.85 % accuracy and 0.9952 AUC performance parameters in differentiating seizure and nonseizure states. Furthermore, considering the low resampling frequency (e.g., 64 Hz) and the use of feature reduction, this study is important in terms of storage space and processing speed performance.

ACKNOWLEDGMENT

The authors sincerely thank the critics for their time and effort in this research work, as well as for their constructive suggestions to the study.

CONFLICTS OF INTEREST

The authors declare that they have no conflicts of interest.

REFERENCES

[1] M. S. Muñoz, C. E. S. Torres, R. Salazar-Cabrera, D. M. López, and R. Vargas-Cañas, "Digital transformation in epilepsy diagnosis using raw images and transfer learning in electroencephalograms", *Sustainability*, vol. 14, no. 18, p. 11420, 2022. DOI: 10.3390/su141811420.

[2] A. Fine and E. C. Wirrell, "Seizures in children", *Pediatr. Rev.*, vol. 41, no. 7, pp. 321–347, 2020. DOI: 10.1542/pir.2019-0134.

[3] E. M. Mizrahi, "Pediatric electroencephalographic video monitoring", *Journal of Clinical Neurophysiology*, vol. 16, no. 2, pp. 100–110, 1999. DOI: 10.1097/00004691-199903000-00002.

[4] K. Pal and B. V. Patel, "Data classification with k-fold cross validation and holdout accuracy estimation methods with 5 different machine learning techniques", in *Proc. of 2020 Fourth International Conference on Computing Methodologies and Communication (ICCMC)*, 2020, pp. 83–87. DOI: 10.1109/ICCMC48092.2020.ICCMC-00016.

[5] M. Eberlein *et al.*, "Convolutional neural networks for epileptic seizure prediction", in *Proc. of 2018 IEEE International Conference on Bioinformatics and Biomedicine (BIBM)*, 2018, pp. 2577–2582. DOI: 10.1109/BIBM.2018.8621225.

[6] P. K. Sethy, M. Panigrahi, K. Vijayakumar, and S. K. Behera, "Machine learning based classification of EEG signal for detection of child epileptic seizure without snipping", *Int. J. Speech Technol.*, vol. 26, pp. 559–570, 2023. DOI: 10.1007/s10772-021-09855-7.

[7] E. Por, M. van Kooten, and V. Sarkovic, "Nyquist–Shannon sampling theorem", Leiden University, 2019.

[8] J. Malmivuo and R. Plonsey, *Bioelectromagnetism: Principles and Applications of Bioelectric and Biomagnetic Fields*. Oxford University Press, New York, 1995. DOI: 10.1093/acprof:oso/9780195058239.001.0001.

[9] S. Mahmud, M. S. Hossain, M. E. H. Chowdhury, and M. B. I. Reaz, "MLMRS-Net: Electroencephalography (EEG) motion artifacts removal using a multi-layer multi-resolution spatially pooled 1D signal reconstruction network", *Neural Comput & Applic.*, vol. 35, pp. 8371–8388, 2023. DOI: 10.1007/s00521-022-08111-6.

[10] S. A. Taywade and R. D. Raut, "A review: EEG signal analysis with different methodologies", in *Proc. of National Conference on Innovative Paradigms in Eng. and Tech.*, 2012, pp. 29–31.

[11] K. Zeng, J. Yan, Y. Wang, A. Sik, G. Ouyang, and X. Li, "Automatic detection of absence seizures with compressive sensing EEG", *Neurocomputing*, vol. 171, pp. 497–502, 2016. DOI: 10.1016/j.neucom.2015.06.076.

[12] M. Congedo, C. Özen, and L. Sherlin, "Notes on EEG resampling by natural cubic spline interpolation", *Journal of Neurotherapy*, vol. 6, no. 4, pp. 73–80, 2002. DOI: 10.1300/J184v06n04_08.

[13] M. Klug *et al.*, "The BeMoBIL Pipeline for automated analyses of multimodal mobile brain and body imaging data", BioRXiv: The Preprint Server for Biology, 2022. DOI: 10.1101/2022.09.29.510051.

[14] P. C. Reddy, V. S. S. P. Tej, A. Siripuram, and B. Osgood, "Computing the Discrete Fourier transform of signals with spectral frequency support", in *Proc. of 2021 IEEE International Symposium on Information Theory (ISIT)*, 2021, pp. 2381–2386. DOI: 10.1109/ISIT45174.2021.9518104.

[15] M. F. Wahab, F. Gritti, and T. C. O'Haver, "Discrete Fourier transform techniques for noise reduction and digital enhancement of analytical signals", *TrAC Trends in Analytical Chemistry*, vol. 143, art. 116354, 2021. DOI: 10.1016/j.trac.2021.116354.

[16] R. N. Bracewell, *The Fourier Transform and its Applications*, 3rd ed., McGraw-Hill, New York, 2000.

[17] W. L. Briggs and V. E. Henson, *The DFT: An Owner's Manual for the Discrete Fourier Transform*. Society for Industrial and Applied Mathematics, 1995.

[18] J. Cooley, P. Lewis, and P. Welch, "Application of the fast Fourier transform to computation of Fourier integrals, Fourier series, and convolution integrals", *IEEE Trans. Audio Electroacoust*., vol. 15, no. 2, pp. 79–84, 1967. DOI: 10.1109/TAU.1967.1161904.

[19] A. Phinyomark, P. Phukpattaranont, and C. Limsakul, "Feature reduction and selection for EMG signal classification", *Expert Systems with App.*, vol. 39, no. 8, pp. 7420–7431, 2012. DOI: 10.1016/j.eswa.2012.01.102.

[20] M. A. Oskoei and H. Hu, "Support vector machine-based classification scheme for myoelectric control applied to upper limb", *IEEE Transactions on Biomedical Engineering*, vol. 55, no. 8, pp. 1956–1965, 2008. DOI: 10.1109/TBME.2008.919734.

[21] A. Krenker, J. Bešter, and A. Kos, "Introduction to the artificial neural networks", in *Artificial Neural Networks: Methodological Advances and Biomedical Applications*. IntechOpen, 2011, pp. 1–18. DOI: 10.5772/15751.

[22] N. Nazmi, M. A. A. Rahman, S.-I. Yamamoto, and S. A. Ahmad, "Walking gait event detection based on electromyography signals using artificial neural network", *Biomedical Signal Processing and Control*, vol. 47, pp. 334–343, 2019. DOI: 10.1016/j.bspc.2018.08.030.

[23] D. P. Kingma and J. Ba, "Adam: A method for stochastic optimization", 2017. DOI: 10.48550/arXiv.1412.6980.

[24] H. Liu, "Rail transit channel robot systems", in *Robot Systems for Rail Transit Applications*. Elsevier, Inc., 2020, pp. 283–328. DOI: 10.1016/B978-0-12-822968-2.00007-3.

[25] M. Teplan, "Fundamental of EEG measurement", *Measurement Science Review*, vol. 2, pp. 1–11, 2002.

[26] G. C. Cardarilli *et al.*, "A pseudo-softmax function for hardware-based high speed image classification", *Scientific reports*, vol. 11, art. no. 15307, 2021. DOI: 10.1038/s41598-021-94691-7.

[27] R. Oostenveld, P. Fries, E. Maris, and J.-M. Schoffelen, "Fieldtrip: Open source software for advanced analysis of MEG, EEG, and invasive electrophysiological data", *Comput. Intell. Neurosci.*, vol. 2011, art. ID 156869, pp. 1–9, 2011. DOI: 10.1155/2011/156869.

[28] A. N. Kamarudin, T. Cox, and R. Kolamunnage-Dona, "Time-dependent ROC curve analysis in medical research: Current methods and applications", *BMC Med. Res. Methodology*, vol. 17, art. no. 53, 2017. DOI: 10.1186/s12874-017-0332-6.

[29] J. Too, A. R. Abdullah, N. M. Saad, and W. Tee, "EMG feature selection and classification using a pbest-guide binary particle swarm optimization", *Computation*, vol. 7, no. 1, p. 12, 2019. DOI: 10.3390/computation7010012.

[30] J. Gu *et al.*, "Recent advances in convolutional neural networks", *Pattern Recognition*, vol. 77, pp. 354–377, 2018. DOI: 10.1016/j.patcog.2017.10.013.

[31] L. J. Goncales, K. Farias, L. Kuppsinsku, and M. Segalotto, "The effects of applying filters on EEG signals for classifying developers' code comprehension", *Journal of Applied Research and Technology*, vol. 19, no. 6, pp. 584–602, 2021. DOI: 10.22201/icat.24486736e.2021.19.6.1299.

[32] L. V. Tran, H. M. Tran, T. M. Le, T. T. M. Huynh, H. T. Tran, and S. V. T. Dao, "Application of machine learning in epileptic seizure detection", *Diagnostics*, vol. 12, no. 11, p. 2879, 2022. DOI: 10.3390/diagnostics12112879.